

## Article

# Investigation and Optimisation of the Rheological Properties of Magnesium Potassium Phosphate Cement with Response Surface Methodology

Yanfei Yue <sup>1,\*</sup>, Jun Ren <sup>2,3</sup>, Kai Yang <sup>1,4</sup>, Danqian Wang <sup>1,3</sup>, Jueshi Qian <sup>1</sup> and Yun Bai <sup>3,\*</sup>

<sup>1</sup> College of Materials Science and Engineering, Chongqing University, 174 Shazheng Street, Shapingba, Chongqing 400044, China

<sup>2</sup> School of Architecture and Planning, Yunnan University, Kunming 650051, China

<sup>3</sup> Department of Civil, Environmental and Geomatic Engineering, University College London, Gower Street, London WC1E 6BT, UK

<sup>4</sup> School of Civil Engineering, University of Leeds, Woodhouse Lane, Leeds LS2 9JT, UK

\* Correspondence: yanfei.yue@cqu.edu.cn (Y.Y.); yun.bai@ucl.ac.uk (Y.B.)

**Abstract:** Magnesium phosphate cement (MPC) is a promising alternative cement. However, the rheological property of this new binder is still to be explored. In this study, Response Surface Methodology (RSM) was adopted with Central Composite Design (CCD) to establish mathematical models describing the rheological characteristics of MPC in terms of initial mini slump ( $Y_1$ ), mini-slump loss ( $Y_2$ ), yield stress ( $Y_3$ ) and plastic viscosity ( $Y_4$ ), as a function of three independent variables, namely, water-to-solid ratio (W/S ratio,  $X_1$ ), MgO to MKP ratio (M/P ratio,  $X_2$ ) and borax dosage ( $X_3$ ). The results show that the M/P ratio and borax dosage could significantly affect the yield stress and mini-slump loss of MPC, while the W/S ratio was the significant coefficient influencing plastic viscosity and initial mini slump. The numerical optimised values of  $X_1$ ,  $X_2$  and  $X_3$  were 0.280, 7.528 and 0.170, respectively, and an MPC paste with desirable rheological characteristics ( $Y_1$  161.858 mm,  $Y_2$  11.282,  $Y_3$  0.680 Pa,  $Y_4$  0.263 Pa·s) with the highest desirability of 0.867 can be obtained.

**Keywords:** magnesium potassium phosphate cement; mini slump; plastic viscosity; response surface methodology; rheological properties; yield stress



**Citation:** Yue, Y.; Ren, J.; Yang, K.; Wang, D.; Qian, J.; Bai, Y.

Investigation and Optimisation of the Rheological Properties of Magnesium Potassium Phosphate Cement with Response Surface Methodology.

*Materials* **2022**, *15*, 6815. <https://doi.org/10.3390/ma15196815>

Academic Editor: A. Javier Sanchez-Herencia

Received: 12 May 2022

Accepted: 21 September 2022

Published: 30 September 2022

**Publisher's Note:** MDPI stays neutral with regard to jurisdictional claims in published maps and institutional affiliations.



**Copyright:** © 2022 by the authors. Licensee MDPI, Basel, Switzerland. This article is an open access article distributed under the terms and conditions of the Creative Commons Attribution (CC BY) license (<https://creativecommons.org/licenses/by/4.0/>).

## 1. Introduction

Magnesium phosphate cement (MPC), also known as chemically bonded phosphate ceramic, is an alternative clinker-free binder which has attracted increasing attention worldwide [1–5]. Compared to the traditional cement [6], MPC possesses many superior properties, such as super-fast setting, high early strength, strong bonding, low drying shrinkage and better durability [1–5]. These properties make MPC remarkably popular in the fast repair, strengthening and rehabilitation of concrete infrastructures such as pavements, highways and airport runways [7,8]. In recent decades, MPC has also demonstrated huge potential for stabilising/solidifying heavy metals, immobilising nuclear wastes, as well as 3D-printing [9,10]. As a promising alternative cement, the hydration and hardening mechanisms of MPC have been extensively studied in the past [11–14]. In general, the hydration of MPC is considered to be a through-solution acid-base exothermic reaction between dead-burnt magnesia (MgO) and an acid phosphate source in the presence of water to form magnesium phosphate hydrates [11–14]. Although monoammonium phosphate ( $\text{NH}_4\text{H}_2\text{PO}_4$ , MAP) has widely been employed as the source of phosphate in earlier studies in the literature, monopotassium phosphate ( $\text{KH}_2\text{PO}_4$ , MKP) has increasingly been employed in recent years owing to its lower solubility than ammonium phosphates, which can slow down the violent reaction and reduce the heat released. Additionally, using MKP also has the advantage of avoiding the emission of unpleasant ammonium gas [14]. The

main hydration product of the MgO–KH<sub>2</sub>PO<sub>4</sub> system is MgKPO<sub>4</sub>·6H<sub>2</sub>O (k-struvite), and its composition and structure are reported to be analogous to those of NH<sub>4</sub>MgPO<sub>4</sub>·6H<sub>2</sub>O (struvite) formed in the MgO–NH<sub>4</sub>H<sub>2</sub>PO<sub>4</sub> system [5,14,15]. Different from the poorly ordered calcium silicate hydrate (C-S-H) gel formed in PC, the magnesium phosphate hydrates formed in MPC are mainly crystalline phases, and thus, its volume stability is believed to be better than PC-based materials [16,17].

Although the fundamentals regarding MPC—such as its hydration mechanisms, the properties of the hydrates, factors affecting the properties, as well as its potential applications—have been extensively investigated [13,14,18,19], its rheological properties are rarely reported and largely unknown. Whilst the rheological properties of conventional PC-based cementitious materials have been well established and commonly described using a Bingham model defined by yield stress ( $\tau$ ) and plastic viscosity ( $\mu$ ) [20], studying the rheological properties of MPC could be rather challenging. This could partly be due to its super-fast setting, making it extremely difficult to characterise its fresh properties, such as rheology. Nonetheless, to efficiently utilise MPC-based materials in industrial applications, their rheological behaviour needs to be understood and optimised. This will also significantly benefit the transporting, placing, and finishing processes in engineering practice. Apart from its super-fast setting, the two main constituents of MPC could also cause complex issues to the fresh properties of MPC. This is because, even though the water-to-solid (W/S) ratio is widely established and expected to affect the rheology of MPC system, the MgO to MKP (M/P) ratio can also cause uncertainties to the properties of MPC. For example, it has been shown that the compressive strength of MPC is not a simple monotonic function of M/P. Instead, at a given W/S, there is always an optimal M/P for the highest compressive strength [8], which is different from what has been widely anticipated, i.e., the higher the M/P, the higher the compressive strength. In terms of rheology, whether such kinds of complex also exist is still unknown in the literature. Furthermore, except for the MgO and phosphate salt, a ‘third’ part, termed as retarder, is usually incorporated in the manufacture of MPC to modulate the setting time. This retarding agent, normally boric acid (H<sub>3</sub>BO<sub>3</sub>) or borate (Na<sub>2</sub>B<sub>4</sub>O<sub>7</sub>·5H<sub>2</sub>O), could introduce further uncertainty and complexity to the fresh properties of MPC [12,21]. Due to the above issues, performance-based design approaches have been widely adopted by different researchers to obtain the desired strength properties. Although this trial-error based method has also been extensively used in the laboratory to formulate the MPC with targeted fresh properties, it is not only time-consuming, but also resource-intensive. Moreover, even though this performance-based approach could allow a mix with good performance to be identified, it cannot ensure a mix with the optimal performance being always achieved. Therefore, Response Surface Methodology (RSM) is attempted as a potential mathematical tool in this paper to resolve the above complexes in order to optimise the rheological properties of MPC based on systematic numerical analyses.

Response Surface Methodology (RSM) is a mathematical and statistical approach using empirical modelling to explore the relationships between independent variables (explanatory factors) and the responses of interests, as well as the interactions between the independent variables [22]. Compared to the standard experimental methods, RSM makes a research strategy systematic and efficient to correlate the interactive effects of numerous parameters simultaneously with the help of statistical procedures. The Central Composite Design (CCD) is the most used surface response statistical design method, which runs much fewer experiments than a full factorial design but provides almost the same information [23]. Hence, the RSM jointly used with the statistic design method (e.g., CCD) is recognised as a significant approach in the design and optimisation process, which has also recently been effectively employed to investigate the interactive effects of independent variables in many areas [24–26]. In the field of cement and concrete research, RSM demonstrated great potential for experimental optimisation, particularly in optimising the rheological parameters, hydration and mechanical properties of cementitious materials [27–30]. Recently, Hou et al. [31] presented their research on optimising the

setting time and early-age compressive strength of MPC cement with RSM methodology for rapid repair applications. Using water-to-binder ratio, magnesia-to-phosphate ratio and borax content as the variables, and the setting time and early-age compressive strength as the responses in RSM, a statistical model was successfully developed by Hou et al. [31], showing a good potential of applying RSM for the design and optimisation of MPC mix. However, the rheological parameters (e.g., mini slump, mini-slump loss, yield stress and plastic viscosity) of MPC were not investigated in their study.

Building upon the aforementioned information, it is anticipated that RSM-CCD methodology could be used to explore the rheological property of this new MPC materials. Hence, in this study, the RSM methodology was adopted to investigate the rheological behaviour of MPC material and also to optimise the mix proportion in terms of water/solid ratio (W/S), MgO/MKP ratio (M/P) and borax dosage, with initial mini slump, mini-slump loss, yield stress ( $\tau$ , Pa) and plastic viscosity ( $\mu$ , Pa·s) considered as responses. The CCD design was, therefore, conducted to develop a three variables (factors) ( $n = 3$ ) experiment matrix with 20 runs in total. In addition, the analysis of variance (ANOVA) was conducted to assess the significance and adequacy of the regression models attained. Finally, to supplement the mathematical analyses, the early-age (i.e., 1 d and 7 d) compressive strength of the MPC pastes was investigated to verify its application in real engineering practices.

## 2. Materials and Methods

### 2.1. Materials

Magnesium oxide (MgO) provided by Richard Baker Harrison Ltd., Manchester, UK, was a Dead Burned Magnesite (DBM) calcined at about 1750 °C with a purity of 90% and a mesh size of 200  $\mu\text{m}$ . Monopotassium phosphate ( $\text{KH}_2\text{PO}_4$ , MKP) was a food-grade MKP with a specified purity >99%, from Prayon UK. Sodium tetraborate decahydrate (borax,  $\text{Na}_2\text{B}_4\text{O}_7 \cdot 10\text{H}_2\text{O}$ ), supplied by Sigma-Aldrich US, was employed as the retarder. It was ACS reagent grade with assay  $\geq 99.5\%$  and a pH of 9.15–9.20.

### 2.2. Design and Sample Preparation

The work process contains three steps: (1) selecting targeted performance parameters and key influencing factors; (2) building and fitting the statistical models for each performance parameter; (3) optimising the mix proportion to achieve the aimed performance. The overall framework for this study is illustrated in Figure 1.

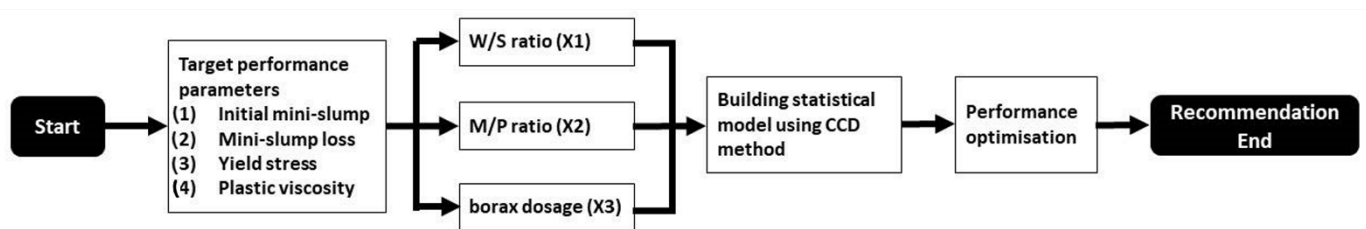


**Figure 1.** Illustration of overall experimental design for this study.

A typical CCD design involves  $2^n$  factorial points,  $2^n$  axial points, and  $n_c$  centre points, in which  $n$  represents the number of factors/variables, and the  $n_c$  refers to the number of repetitions of the centre point. The repetition of the central point is to estimate the experimental internal error and, thus, to improve the reliability of the models. In this study, a  $2^3$  CCD design with three variables ( $n = 3$ ) and two extreme levels (coded as  $+\alpha$  and  $-\alpha$ ) was applied to develop the mathematical equation and quantify the rheological properties of MPC in terms of initial mini slump, mini-slump loss, yield stress and plastic viscosity. The three variables investigated in this study were water/solid ratio (W/S) ( $X_1$ ), MgO/MKP ratio (M/P) ( $X_2$ ) and borax dosage ( $X_3$ ) (by the weight of MgO). A total of 20 runs, including eight ( $2^n = 2^3$ ) factorial points, six ( $2n = 2 \times 3$ ) axial points and six (replicates) centre points, were carried out. The CCD design and data analysis associated

with the analysis of variance (ANOVA) and RSM optimisation were conducted using Design Expert 10 (Stat-Ease, Minneapolis, MN, USA) software. Table 1 below reports the actual values of the factors, and Figure 2 visually illustrates the distribution of the coded points for the designed matrix. It should be noted that the ranges/levels of the variables were determined based on the results from our previous work [32]. In total, 20 MPC pastes were designed by the CCD method and the details of the coded value of mixing portions are given in Table 2.

Table 1. Actual values for the variables used in the experimental design.

Independent Variables	Symbols	Actual Values for the Coded Values				
		$-\alpha (-1.682)$	$-1$	$0$	$+1$	$+\alpha (+1.682)$
W/S ratio	$X_1$	0.18	0.20	0.24	0.28	0.30
M/P ratio	$X_2$	2	4.03	7	9.97	12
borax dosage	$X_3$	0.13	0.14	0.16	0.17	0.18

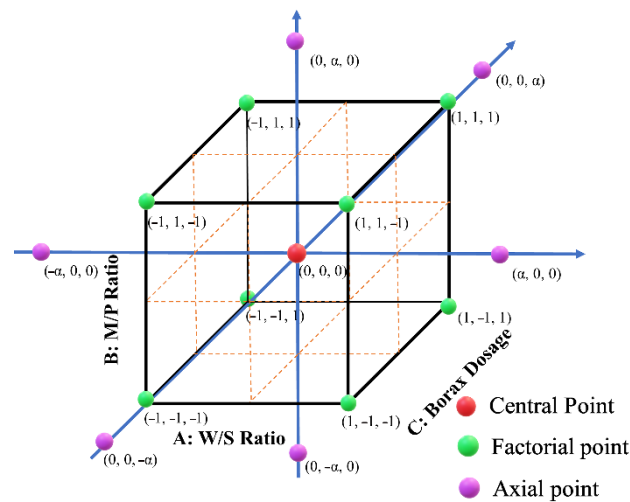


Figure 2. Schematic of the design points with coded values.

Table 2. The points for 3 factors CCD design (coded value).

Runs	W/S Ratio ( $X_1$ )	M/P Ratio ( $X_2$ )	Borax Dosage ( $X_3$ )
1	0	0	0
2	-1	1	-1
3	0	0	1.682
4	0	0	0
5	0	0	0
6	-1	-1	-1
7	-1.682	0	0
8	0	0	-1.682
9	1.682	0	0
10	1	1	-1
11	0	0	0
12	1	-1	1
13	-1	1	1
14	-1	-1	1
15	0	-1.682	0
16	0	0	0
17	1	1	1
18	0	0	0
19	1	-1	-1
20	0	1.682	0

All 20 MPC pastes, as shown in Table 2, were fabricated in a high-shear mixer. The borax was first mixed with water and followed by adding MKP and MgO. The total mixing time was 3 min.

### 2.3. Test Methods

#### 2.3.1. Rheological Properties Test

Immediately after mixing, the pastes were transferred into the container (92 mm diameter) of a modified and calibrated rheometer, which uses a helical impeller to establish the relationship between shear stress and shear rate. The results were recorded by the software and the yield stress and plastic viscosity were fitted by the Bingham model. The mini-slump test was conducted with a conical mould with a lower inner diameter of 38.1 mm, an upper inner diameter of 19 mm and a height of 57.1 mm. The mini slump was determined at 15 min and 45 min after mixing. The mini-slump loss was then calculated as the difference between the values of mini slump at 15 min and 45 min.

#### 2.3.2. Compressive Strength Test

The  $25 \times 25 \times 25$  mm<sup>3</sup> PVC moulds were used to cast cubes to determine the compressive strength of the paste. Immediately after mixing, the moulds were filled with the paste and a steel scraper was used to finish the specimen surface. The moulds were covered with water-saturated hessian and stored in a constant temperature room at  $20 \pm 1$  °C for 24 h. The specimens were then demoulded, and each cube was wrapped with a water-saturated hessian before being sealed in an air-tight plastic bag. The specimens were again stored in the same constant-temperature room until being tested.

### 2.4. Data Analysis

The data were processed by Design Expert software. The analysis of variance (ANOVA) with Fisher's F-test was conducted to check the significance and adequacy of the models established. The desirability function (DF) approach was used to establish the optimum criteria based on multi-variables. The general procedure of this approach is to convert each response  $Y_k$  into an individual desirability function as  $d_k = f(Y_k)$  ( $0 \leq d_k \leq 1$ ). If the response ( $Y_k$ ) meets the target of the optimisation goal,  $d_k$  is then valued as 1; while the response is beyond the acceptable limit, then  $d_k$  is 0.

## 3. Results and Discussion

### 3.1. Model Adequacy Analysis

The experimental data in terms of the four responses (i.e.,  $Y_1$ ,  $Y_2$ ,  $Y_3$  and  $Y_4$ ) obtained from all 20 mixes are presented in Table 3 and analysed by Design Expert 10. The best-fitting surface response model for describing the mini slump ( $Y_1$ ) is generated, which is suggested to be a linear relation, whilst the models of the other three responses, i.e., mini-slump loss ( $Y_2$ ), yield stress ( $Y_3$ ), and plastic viscosity ( $Y_4$ ), are two-factor interactions (2FI). The regression equations in the coded value attained correlating to the responses and the three independent variables are shown in Equations (1)–(4) for initial mini slump, mini-slump loss, yield stress and plastic viscosity, respectively. The analysis of variance (ANOVA) with Fisher's F-test was then conducted to assess the significance and adequacy of these models, which are reported and discussed in separate sections (Sections 3.1.1–3.1.5) below. Since the repeatability of the responses at the central points was used for estimating the error of the models, the analysis of the results of the four responses at central points was also conducted, and the results are presented in Table 4.

$$Y_1 = 153.60 + 9.48X_1 + 0.14X_2 - 1.24X_3 \quad (1)$$

$$Y_2 = 38.75 - 9.84X_1 + 28.68X_2 - 13.55X_3 + 3.87X_1X_2 - 5.62X_1X_3 - 23.88X_2X_3 \quad (2)$$

$$Y_3 = 9.61 - 9.67X_1 + 11.60X_2 - 10.41X_3 - 14.25X_1X_2 + 14.33X_1X_3 - 15.23X_2X_3 \quad (3)$$

$$Y_4 = 0.73 - 0.43X_1 - 0.04X_2 + 0.20X_3 + 0.24X_1X_2 - 0.37X_1X_3 + 0.52X_2X_3 \quad (4)$$

**Table 3.** The points for 3 factors CCD design (coded value) and corresponding responses.

Runs	Variables in Coded Values			Responses			
	W/S Ratio (X <sub>1</sub> )	M/P Ratio (X <sub>2</sub> )	Borax Dosage (X <sub>3</sub> )	Initial Mini Slump/mm (Y <sub>1</sub> )	Mini-Slump Loss (Y <sub>2</sub> )	Yield Stress/Pa (Y <sub>3</sub> )	Plastic Viscosity/Pa·s (Y <sub>4</sub> )
1	0	0	0	159	33	2.03	0.77
2	−1	1	−1	140	102	122.65	−1.47
3	0	0	1.682	156	22	1.18	0.59
4	0	0	0	152	22	1.76	0.70
5	0	0	0	155	25	1.39	0.74
6	−1	−1	−1	142	12	3.57	1.42
7	−1.682	0	0	134	96	7.38	3.00
8	0	0	−1.682	156	22	10.96	0.81
9	1.682	0	0	164	6	1.17	0.36
10	1	1	−1	175	137	7.18	0.37
11	0	0	0	168	36	1.46	0.66
12	1	−1	1	155	10	0.68	0.33
13	−1	1	1	144	31	4.20	2.10
14	−1	−1	1	143	13	1.84	0.90
15	0	−1.682	0	156	23	0.98	0.31
16	0	0	0	161	31	1.13	0.69
17	1	1	1	158	20	1.85	0.46
18	0	0	0	147	17	1.40	0.72
19	1	−1	−1	160	8	0.90	0.31
20	0	1.682	0	147	109	18.50	0.88

**Table 4.** Repeatability of the responses at central points.

Test	Initial Mini Slump /mm	Mini-Slump Loss	Yield Stress /Pa	Plastic Viscosity /Pa·s
Mean (n = 6)	157.00	27.33	1.53	0.71
Standard Derivation	7.35	7.23	0.32	0.04
Standard Error	3.00	2.95	0.13	0.02
Coefficient of Variation (%)	4.68	26.45	20.78	5.44

### 3.1.1. Analysis of Variance (ANOVA) of the Response Model of Initial Mini-Slump

The analysis of variance of the model of initial mini slump (Equation (1)) is shown in Table 5. The obtained F-value of 9.67 and p-value of 0.0007 (<0.05) implies that the regression model was highly significant at a 5% significance level, and there was only a 0.07% chance that an F-value this large could occur due to noise. The goodness of fit of the model was assessed by the coefficient of determination R<sup>2</sup> and equalled to 0.6446, which indicates that about 64.46% of the variation in this system was attributed to the independent variables, and only about 35% of the variation could not be explained by the model. In addition, the adequate precision value measures the signal-to-noise ratio and a value greater than 4 is desirable. The value obtained from the current model was 10.8699, suggesting that the adequate signal was obtained, and this model can be used to navigate the design space. Moreover, the significance of each of the coefficients can be checked by the p-value, as listed in Table 5, and p < 0.05 could suggest that the term is significant. From our results, evidently, the X<sub>1</sub> is the significant model term. This suggests that the factor W/S (X<sub>1</sub>) is the most significant term for the linear model of mini slump, which significantly affects the initial mini slump of the MPC paste.

**Table 5.** Analysis of variance (ANOVA) of the response model of initial mini-slump.

Source	Responses				
	Initial Mini-Slump ( $Y_1$ )				
	Sum of Squares	DF	MS	F-Value	p-Value (Prob > F)
Model	1248.51	3	416.17	9.67	0.0007
$X_1$	1227.10	1	1227.10	28.53	0.0001
$X_2$	0.25	1	0.25	0.01	0.9397
$X_3$	21.16	1	21.16	0.49	0.4931
Residual	688.29	16	43.02		
Lack of fit	418.29	11	38.03	0.70	0.7090
Pure Error	270.00	5	54.00		
Cor Total	1936.80	19			
$R^2$			0.6446		
Adeq			10.8699		
Precision					

### 3.1.2. Model Describing Mini-Slump Loss

Similarly, the ANOVA analysis with Fisher's F-test was conducted to check the significance and adequacy of the model of mini-slump loss (Equation (2)), which is presented in Table 6. The F-value and p-value of the 2FI model were 5.18 and 0.0063, respectively, revealing that the model was significant. Moreover, the coefficient of determination (goodness of fit) was  $R^2 = 0.7051$ , which indicates that 70.51% of the variation in this system can be attributed to the independent variables. In addition, the value of adequate precision was 7.6423, which suggests that the model can be validly used in the examined range of experiments. Moreover, by checking the p-value of all the terms, the factors of  $X_2$  (0.0011) as well as  $X_2X_3$  (0.0195) were significant model terms, which suggests that M/P ( $X_2$ ) significantly affects the mini-slump loss of MPC (95% confidence limit), and there are significant interactions between M/P and borax dosage ( $X_2X_3$ ). On the other hand, the factor borax dosage ( $X_3$ ) was still within the 90% confidence limit, which also somehow showed the influence on the mini-slump loss of MPC.

**Table 6.** Analysis of variance (ANOVA) of the response model of mini-slump loss.

Source	Responses				
	Mini-Slump Loss ( $Y_2$ )				
	Sum of Squares	DF	MS	F-Value	p-Value (Prob > F)
Model	19,992.14	6	3332.02	5.18	0.0063
$X_1$	1321.90	1	1321.90	2.06	0.1753
$X_2$	11,230.80	1	11,230.80	17.46	0.0011
$X_3$	2506.07	1	2506.07	3.90	0.0700
$X_1X_2$	120.13	1	120.13	0.19	0.6727
$X_1X_3$	253.13	1	253.13	0.39	0.5413
$X_2X_3$	4560.13	1	4560.13	7.09	0.0195
Residual	8361.61	13	643.20		
Lack of fit	8100.28	8	1012.54	19.37	0.0023
Pure Error	261.33	5	52.27		
Cor Total	28,353.75	19			
$R^2$			0.7051		
Adeq			7.6423		
Precision					

### 3.1.3. Model Describing Yield Stress

The statistical significance and adequacy of the response model of yield stress (Equation (3)) were checked, and the results are shown in Table 7. The response model was significant, as evidenced by the F-value and p-value which were 5.13 and 0.0066, respectively. Moreover, the coefficient of determination  $R^2$  equalled to 0.7030 (goodness of fit), indicating that 70.30% of the variation in this system can be attributed to the independent variables, and only about 30% of the variation cannot be explained by the model. The lower value of  $R^2$  could be due to the indirect response (yield stress) from the factors. The value of

adequate precision obtained from the current model was 9.6694 (greater than 4), suggesting that the adequate signal was obtained and this model is valid to navigate the design space. Moreover, by checking and comparing the p-value listed in Table 7, it is evident that all the factors and interactions, excepting W/S ( $X_1$ ), were identified as significant model terms at a 95% confidence limit. Based on the statistical analysis, the M/P ( $X_2$ ) and borax dosage ( $X_3$ ) could significantly affect the yield stress of the MPC materials, and there are significant interactions between W/S and M/P ( $X_1X_2$ ), W/S and borax dosage ( $X_1X_3$ ) and M/P and borax dosage ( $X_2X_3$ ). Furthermore, the p-value of W/S ( $X_1$ ) was 0.0655, which is still acceptable within the allowance of the 90% confidence limit.

**Table 7.** Analysis of variance (ANOVA) of the response model of yield stress.

Source	Responses				
	Yield Stress ( $Y_3$ )				
	Sum of Squares	DF	MS	F-Value	p-Value (Prob > F)
Model	9716.05	6	1619.34	5.13	0.0066
$X_1$	1277.66	1	1277.66	4.05	0.0655
$X_2$	1836.17	1	1836.17	5.82	0.0314
$X_3$	1480.18	1	1480.18	4.69	0.0496
$X_1X_2$	1624.22	1	1624.22	5.14	0.041
$X_1X_3$	1642.51	1	1642.51	5.2	0.0401
$X_2X_3$	1855.32	1	1855.32	5.88	0.0307
Residual	4104.84	13	315.76		
Lack of fit	4104.33	8	513.04	5086.84	<0.0001
Pure Error	0.5	5	0.1		
Cor Total	13,820.88	19			
$R^2$			0.7030		
Adeq			9.6694		
Precision					

#### 3.1.4. Model Describing Plastic Viscosity

The ANOVA analysis for the model of plastic viscosity (Equation (4)) is shown in Table 8. The current model, with a p-value of 0.0979 (which is less than 0.1), could still be considered as significant at a 10% significance level. The determination coefficient  $R^2$  obtained was 0.5151, which suggests that this model can interpret 51.51% of the total variation. Moreover, the adequate signal was retrieved, as evidenced by the adequate precision value of 6.1537. More importantly, the  $X_1$  was observed to be the only significant coefficient in the current model, which implies that the W/S ratio played an important role in adjusting the viscosity of the MPC materials.

**Table 8.** Analysis of variance (ANOVA) of the response model of plastic viscosity.

Source	Responses				
	Plastic Viscosity ( $Y_4$ )				
	Sum of Squares	DF	MS	F-Value	p-Value (Prob > F)
Model	6.84	6	1.14	2.3	0.0979
$X_1$	2.57	1	2.57	5.18	0.0404
$X_2$	0.02	1	0.02	0.04	0.8384
$X_3$	0.57	1	0.57	1.15	0.3030
$X_1X_2$	0.44	1	0.44	0.89	0.3623
$X_1X_3$	1.08	1	1.08	2.18	0.1636
$X_2X_3$	2.16	1	2.16	4.37	0.0569
Residual	6.44	13	0.5		
Lack of fit	6.43	8	0.8	533.79	<0.0001
Pure Error	0.01	5	0.002		
Cor Total	13.28	19			
$R^2$			0.5151		
Adeq			6.1537		
Precision					



### 3.1.5. Summary and Further Improvement

In this section, in addition to the establishment of four prediction models with the analysis factors and their interactions, an ANOVA was carried out, and the influence of the main factors was assessed along with the interaction. For all the models, the p-values were less than 0.1, indicating that these four models are significant at a 10% significance level. Furthermore, based on the analysis of each factor and their interactions, the most significant terms for each model were identified, as discussed in Section 3.2.5. However, two improvements could be further applied: (1) the results indicated strong interactions between the factors affecting mini-slump loss and yield stress, which could be further analysed; (2) the values of  $R^2$  of the four models were below 0.85 and the lowest value was 0.5151, indicating that there is some room to improve these models.

### 3.2. Effect of Variables on the Response of the Model

In this section, based on the statistical analysis of the four predicted models, the effects of different variables and their interactions in each predicted model are discussed.

#### 3.2.1. Effect on Initial Mini-Slump

The 3D response surface plots of the initial mini slump with an interactive relationship between the factors (W/S, M/P, borax dosage) are shown in Figure 3a–c. Based on Equation 1, the initial mini-slump response increased with the increase in the W/S ratio and M/P ratio, whereas it decreased with the increase in borax dosage. Moreover, the higher coefficient of the W/S, which was approximately 67.1 and 7.6 times larger than those of M/P and borax dosage, respectively, indicates that the W/S significantly affected the initial mini slump of MPC. As shown in Figure 3a, the initial mini slump increased with the increase in W/S, whereas the change of the M/P imposed little effect on it. For example, the response of the predicted mini slump was 153.60 mm when the values of W/S and M/P were set as 0.24 and 7, respectively. However, when increasing the W/S to 0.28 while maintaining M/P at 7, the predicted initial mini slump increased to 163.07 mm, while it only increased to 153.73 mm if increasing M/P to 9.97 but keeping the W/S at 0.24. On the other hand, the effects of W/S and borax dosage on the initial mini slump are presented in Figure 3b. Similarly, the initial mini slump increased as the W/S increased towards its high level. In contrast, the initial mini slump decreased along with increasing borax dosage. In addition, as illustrated in Figure 3c, the initial mini slump increased with decreasing borax dosage, while the change in M/P provided little effect on it.

#### 3.2.2. Effect on Mini-Slump Loss

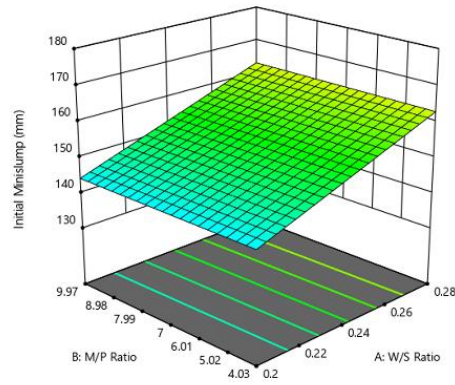
The 3D response surface plots visualizing the effect of the three factors on the mini-slump loss of MPC paste are plotted in Figure 4. Generally, the mini-slump loss response decreased with the increase in W/S and borax dosage, while it increased with the increase in M/P. Moreover, the influences in the order of decreasing magnitude are M/P, borax dosage and W/S. For example, the coefficient of M/P showed an approximately 2.11 times greater effect on the mini-slump loss than the borax dosage (+28.68 vs. −13.55 in Equation (2)). As shown in Figure 4a, while keeping the borax dosage at the middle level (0.16), it is apparent that mini-slump loss decreased with decreasing M/P, whereas it decreased with increasing W/S. Moreover, the combined effects of W/S and borax dosage are shown in Figure 4b. As expected, the mini-slump loss decreased with increasing W/S and borax dosage. Similarly, as shown in Figure 4c, the mini-slump loss decreased with the decrease in M/P and increase in borax dosage. For example, when M/P was 7 and borax dosage was 0.16, the predicted mini-slump loss was 38.75. However, when M/P decreased to 4.03 while maintaining borax dosage at 0.16, the predicted mini-slump loss decreased to 10.23; meanwhile, it also decreased to 25.20 if increasing the borax dosage to 0.17 but keeping the M/P at 7.

Design-Expert® Software  
Factor Coding: Actual

Initial Minislump (mm)  
134  175

X1 = A: W/S Ratio  
X2 = B: M/P Ratio

Actual Factor  
C: Borax dosage = 0.155



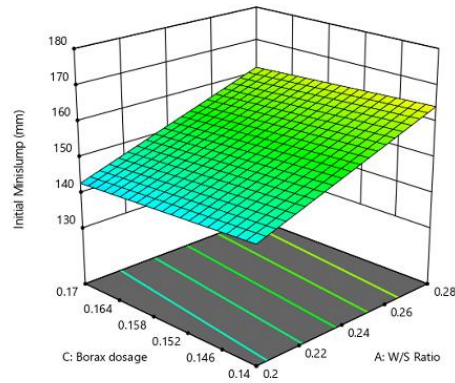
(a)

Design-Expert® Software  
Factor Coding: Actual

Initial Minislump (mm)  
134  175

X1 = A: W/S Ratio  
X2 = C: Borax dosage

Actual Factor  
B: M/P Ratio = 7



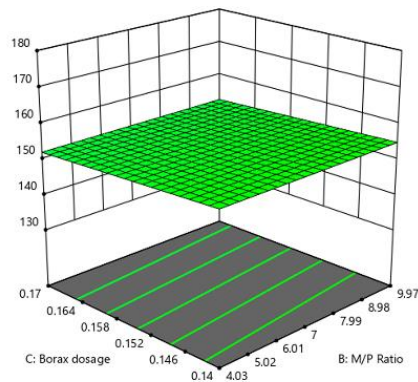
(b)

Design-Expert® Software  
Factor Coding: Actual

Initial Minislump (mm)  
134  175

X1 = B: M/P Ratio  
X2 = C: Borax dosage

Actual Factor  
A: W/S Ratio = 0.24



(c)

Figure 3. Three-dimension response surface plots of initial mini slump ( $Y_1$ ) in relation to: (a) W/S ratio ( $X_1$ ) and M/P ratio ( $X_2$ ); (b) W/S ratio ( $X_1$ ) and borax dosage ( $X_3$ ); (c) M/P ratio ( $X_2$ ) and borax dosage ( $X_3$ ).

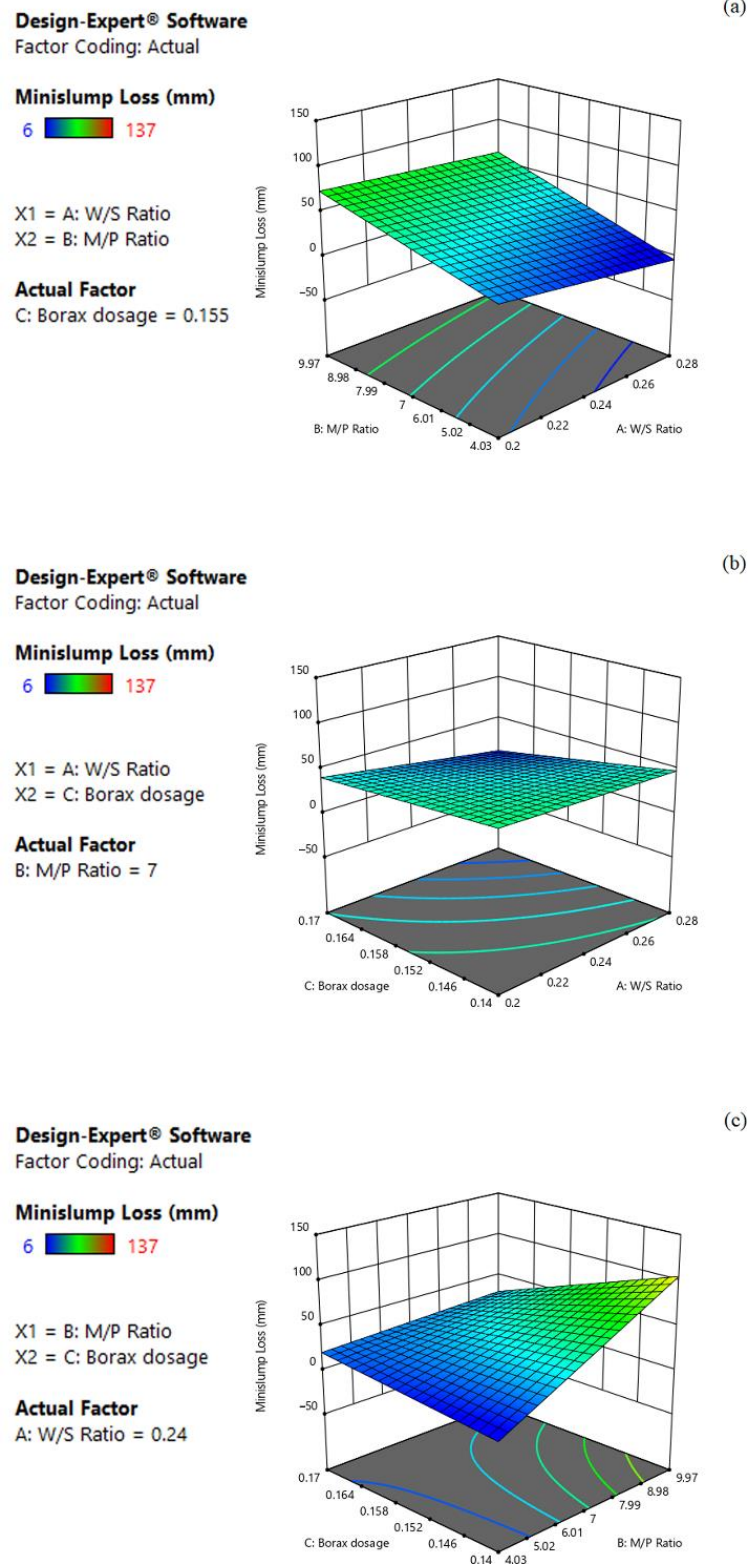


**Figure 4.** Three-dimension response surface plots of mini-slump loss ( $Y_2$ ) in relation to: (a) W/S ratio ( $X_1$ ) and M/P ratio ( $X_2$ ); (b) W/S ratio ( $X_1$ ) and borax dosage ( $X_3$ ); (c) M/P ratio ( $X_2$ ) and borax dosage ( $X_3$ ).

### 3.2.3. Effect on Yield Stress

The 3D response surface plots visualizing the effect of the three factors on the yield stress of MPC paste are plotted as the response surfaces in Figure 5. As shown in Equation (3),

the yield stress response decreased with the increase in W/S and borax dosage, whereas it increased with the increase in M/P. Moreover, the influences in the order of decreasing magnitude are M/P ratio, borax dosage and W/S. For example, the coefficient of M/P showed an approximately 1.2 times greater effect on the yield stress than that of W/S (+11.60 vs. −9.67). As shown in Figure 5a, while keeping the borax dosage at the middle level (0.16), it is evident that the yield stress increased with increasing M/P, whereas it decreased with the increase in W/S. When W/S was 0.24 and M/P was 7, the response of the predicted yield stress value was 9.61 Pa. However, when W/S decreased to 0.20 while maintaining M/P at 7, the predicted yield stress value increased to 19.28 Pa, while it increased to 21.21 Pa if increasing M/P to 9.97 but keeping the W/S at 0.24. The combined effects of W/S and borax dosage are shown in Figure 5b. As expected, the yield stress decreased with increasing W/S and borax dosage. Similarly, as shown in Figure 5c, the yield stress increased with the increase in M/P, while it decreased with increasing borax dosage. There could be interactions between the three factors in relation to the yield stress. For example, the proportion of water could not only affect the fluidity, but also change the hydration process of the MPC [33]. Therefore, further studies still need to be carried out to clarify their roles.

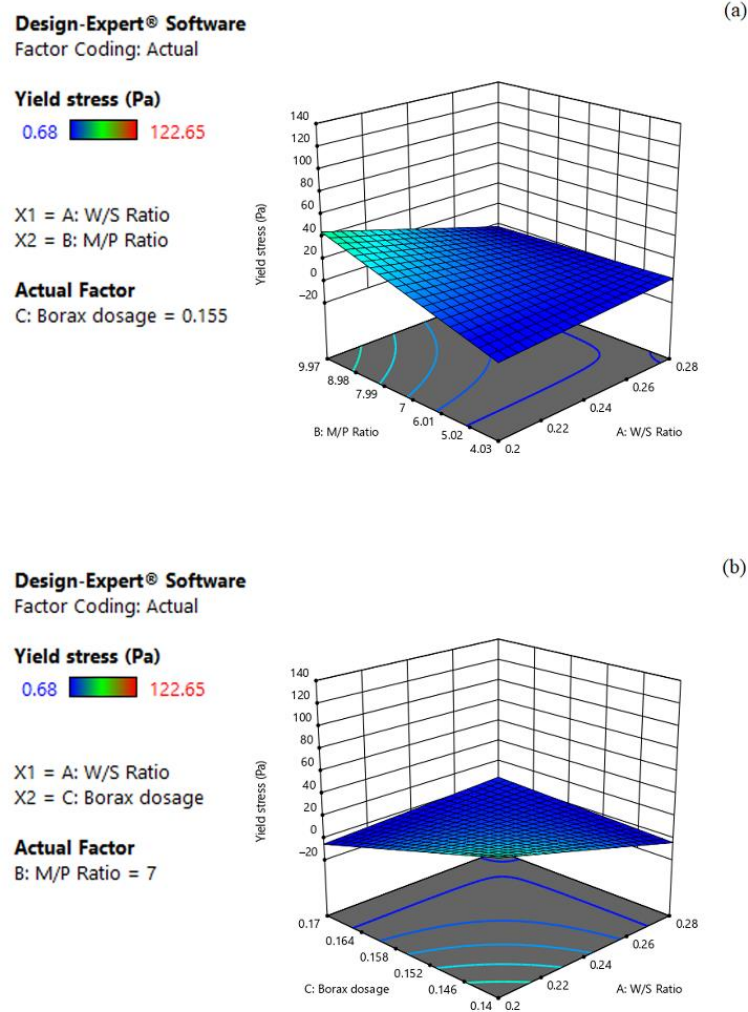
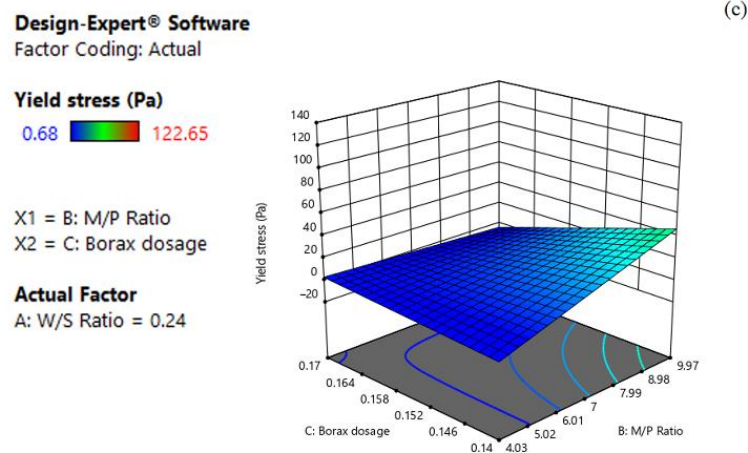


Figure 5. Cont.



**Figure 5.** Three-dimension response surface plots of yield stress ( $Y_3$ ) in relation to: (a) W/S ratio ( $X_1$ ) and M/P ratio ( $X_2$ ); (b) W/S ratio ( $X_1$ ) and borax dosage ( $X_3$ ); (c) M/P ratio ( $X_2$ ) and borax dosage ( $X_3$ ).

### 3.2.4. Effect on Plastic Viscosity

The 3D response surface plots based on Equation 4 are shown in Figure 6a–c. In general, the plastic viscosity response decreased with the increase in the W/S ratio and M/P ratio, while it increased with the increase in borax dosage. Moreover, it is obvious that the coefficient of the W/S ( $-0.43$ ) was approximately 9.8 and 1.2 times higher than that of M/P and borax dosage, respectively, indicating that the W/S can significantly affect the plastic viscosity of MPC. The dependence of plastic viscosity on W/S and M/P for the set of borax dosage at its central level (0.16) is shown in Figure 6a. As can be seen, the plastic viscosity decreased with the increase in W/S, whereas the change in M/P imposed little effect on plastic viscosity. For example, the response of the predicted plastic viscosity was 0.73 Pa·s when the value of W/S and M/P were set as 0.24 and 7, respectively. However, when decreasing the W/S to 0.20 while maintaining the M/P at 7, the predicted plastic viscosity increased to 1.16 Pa·s. However, it only increased to 0.77 Pa·s if decreasing the M/P to 4.03 but keeping the W/S at 0.24. This phenomenon may be attributed to the fact that the change in W/S and MgO proportion could affect the cohesion of the fluids. Additionally, the effects of W/S and borax dosage on the plastic viscosity are presented in Figure 6b. The plastic viscosity decreased as the W/S increased towards its high level, while it increased along with increasing borax dosage. As illustrated in Figure 6c, the plastic viscosity increased with increasing borax dosage, while the change in M/P contributed little to plastic viscosity.

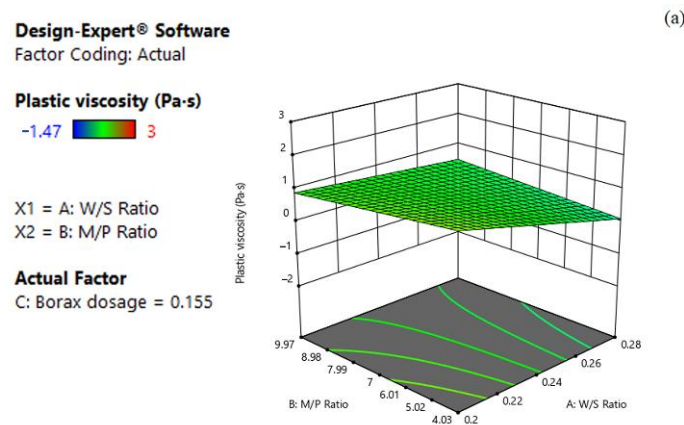


**Figure 6.** Cont.

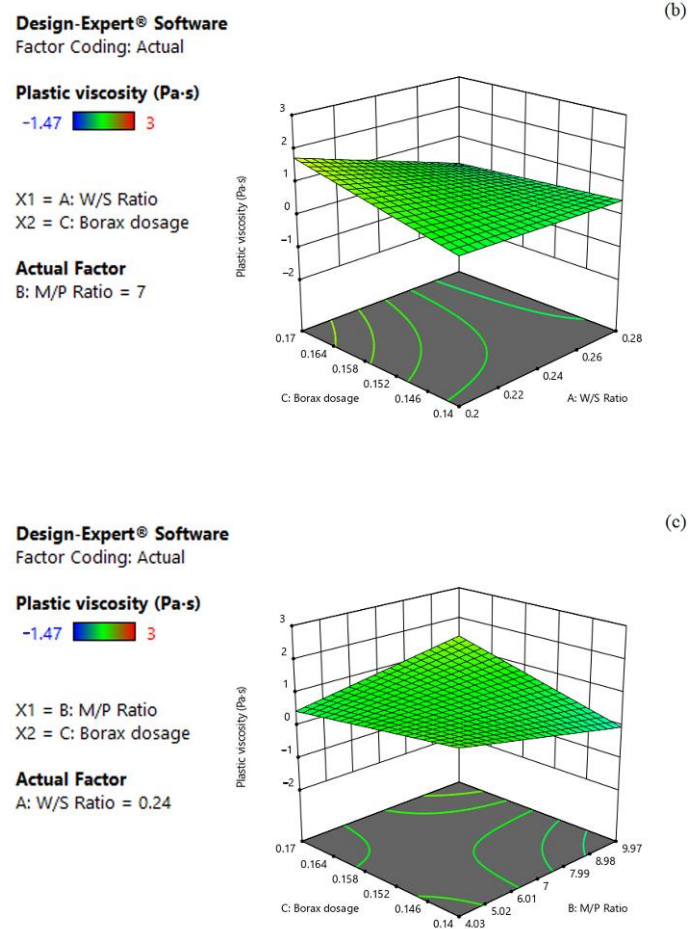


**Figure 6.** Three-dimension response surface plots of plastic viscosity ( $Y_4$ ) in relation to: (a) W/S ratio ( $X_1$ ) and M/P ratio ( $X_2$ ); (b) W/S ratio ( $X_1$ ) and borax dosage ( $X_3$ ); (c) M/P ratio ( $X_2$ ) and borax dosage ( $X_3$ ).

3.2.5. Discussion

To compare the effects of each variable on the rheological behaviour of MPC, the coefficients of all regression models are summarised in Table 9. Since the p-value < 0.05 would indicate that the term is significant at 95% confidence, the significant terms for each response in Table 9 are bold.

**Table 9.** Coefficient table for the variables of all responses.

	Initial Mini Slump		Mini-Slump Loss		Yield Stress		Plastic Viscosity	
	Coefficient	p-Value	Coefficient	p-Value	Coefficient	p-Value	Coefficient	p-Value
Intercept	153.60		38.75		9.61		0.73	
$X_1$	9.48	<0.0001	-9.84	0.1753	-9.67	0.0655	-0.43	<b>0.0404</b>
$X_2$	0.14	0.9397	28.68	<b>0.0011</b>	11.60	<b>0.0314</b>	-0.04	0.8384
$X_3$	-1.24	0.4931	-13.55	0.0700	-10.41	<b>0.0496</b>	0.20	0.3030
$X_1X_2$			3.88	0.6727	-14.25	<b>0.0410</b>	0.24	0.3623
$X_1X_3$			-5.63	0.5413	14.33	<b>0.0401</b>	-0.37	0.1636
$X_2X_3$			-23.88	<b>0.0195</b>	-15.23	<b>0.0307</b>	0.52	0.0569

Note:  $X_1$ : W/S Ratio;  $X_2$ : M/P Ratio;  $X_3$ : borax dosage;  $X_1X_2$ : interaction between W/S ratio and M/P ratio;  $X_1X_3$ : interaction between W/S ratio and borax dosage;  $X_2X_3$ : interaction between M/P ratio and borax dosage.

As shown in Table 9, the W/S ratio mainly affected the initial mini slump and plastic viscosity. The increase in W/S led to the increase in mini slump, but the decrease in plastic viscosity. However, it should be noticed that, although yield stress was not the significant

term at 95% confidence, it was still above the 90% confidence level, indicating that it still can be influenced by W/S. In a cementitious system, Van der Waals interactions have been recognised to dominate all colloidal interactions and, therefore, dictate the inter-particle distance [34]. The increased W/S reduces the concentration of the particles which, therefore, enlarges the inter-particle distance. Since the inter-particles force is inversely proportional to the square of inter-particle distance [35], the increased inter-particle distance due to the high W/S can reduce the inter-particle force. This, in turn, can reduce the formation of the solid network through particle–particle bonds [36]. Consequently, higher mini slump and lower yield stress can be achieved. Moreover, W/S is also identified as the most significant factor influencing the plastic viscosity of MPC. This could be attributed to the fact that the plastic viscosity can somehow reflect the flocculation status in the paste and the resistance to the flow, which in turn, depends on the solid volume fraction and the packed density [37]. The alteration of W/S changed the solid volume, consequently changing the plastic viscosity of MPC.

In terms of the M/P ratio, Table 9 demonstrates that it can significantly affect the mini-slump loss and yield stress. The higher M/P ratio shows a higher mini-slump loss and yield stress. It is well known that the mini-slump loss is closely related to the setting of MPC, whilst the yield stress is closely related to the hydration process. Although it is generally accepted that the main hydration product of MKPC is k-struvite ( $\text{MgKPO}_4 \cdot 6\text{H}_2\text{O}$ ), which is formed from the reaction between MgO and  $\text{KH}_2\text{PO}_4$  [38] through solution, the different ratios between MgO and  $\text{KH}_2\text{PO}_4$  can lead to a different reaction process and products [13]. Specifically, the increased portion of MgO could lead to a higher pH of MPC, which promotes the dissolution of the ions available for reaction [39], and more reaction products could form and precipitate on the particle surface [14]. Consequently, the hydration process could be accelerated and setting time shortened, resulting in a higher mini-slump loss. Furthermore, the produced negatively charged k-struvite or other intermedium products [40,41] from hydration may interact with the positively charged MgO particles [42], which could increase the yield stress by forming the electrostatic attraction force among the particles.

Similarly, borax dosage, another factor which is related to the hydration process, affected the mini-slump loss and yield stress. In contrast to the effect of M/P ratio, the increase in borax dosage reduced both mini-slump loss and yield stress. The addition of borax retarders delayed the setting of MPC [43]. As discussed previously, since the mini-slump loss is linked to the setting of MPC, the increase in the borax dosage reduced the mini-slump loss of MPC by delaying the setting of MPC. Moreover, the addition of borax retards the MPC hydration by formatting the positively charged  $\text{MgB}(\text{OH})_4^+$  complex [43]. Therefore, the electrostatic repulsion between the positively charged complex and MgO could benefit the dispersion of the particles, which can further reduce the yield stress of the MPC paste.

Furthermore, it should be noted that, based on statistical analysis the interaction between any two factors ( $X_1X_2$ ,  $X_1X_3$ ,  $X_2X_3$ ) can still affect the yield stress of the MPC paste. Besides, the interaction between M/P and borax dosage ( $X_2X_3$ ) exhibited a greater influence on mini-slump loss. Such interactions lead to a more complex situation in analysing the fresh property of MPC. Therefore, although the influence of each variable on the fresh property of MPC was discussed in detail, the interactions between these variables need to be further investigated.

### 3.3. Desirability Functions for Numerical Optimisation

Based on the results and the analysis presented in previous sections, the models for all four responses, in terms of initial mini slump, mini-slump loss, yield stress and plastic viscosity (Equations (1)–(4)), were utilised to optimise the best fresh property of MPC paste. Factors including W/S, M/P and borax dosage are involved in the numerical optimisation with the design goal as ‘in range’. On the other hand, the goals in terms of yield stress, plastic viscosity, initial mini slump and mini-slump loss are set as ‘minimised’, ‘in range’,

‘maximised’ and ‘minimised’ to obtain the MPC system with desirable fresh properties. Considering the ease to process the fresh MPC in its future engineering application, the importance of yield stress, initial mini slump and mini-slump loss was set as 5, whereas it was set as 3 (default value) for other terms. The factors and predicted response of the target are listed in Table 10. As shown in the table, the predicted values for the four responses generated from the optimisation are 0.680 Pa (yield stress), 0.263 Pa·s (plastic viscosity), 161.858 mm (initial mini slump) and 11.282 (mini-slump loss), with the highest desirability of 0.867. Accordingly, the optimum conditions of the three variables are 0.280, 7.528 and 0.170 for the W/S, M/P and borax dosage, respectively. Thus, it is anticipated that by following the optimum recipe computed for W/S, M/P and borax dosage, a MPC mix with desirable fresh properties can be obtained. Our paper reported for the first time the optimised rheological parameters of the MPC materials by the statistic RSM-CCD methodology.

**Table 10.** Characteristics of numerical optimisation.

Parameters	Importance	Weight	Goal	Predict Value
W/S Ratio ( $X_1$ )	3	1	In range	0.280
M/P Ratio ( $X_2$ )	3	1	In range	7.528
Borax Dosage ( $X_3$ )	3	1	In range	0.170
Yield Stress/Pa	5	1	Minimise	<b>0.680</b>
Plastic Viscosity/Pa·s	3	1	In range	<b>0.263</b>
Initial Mini Slump/mm	5	1	Maximise	<b>161.858</b>
Mini-Slump Loss	5	1	Minimise	<b>11.282</b>
Desirability			<b>0.867</b>	

### 3.4. Compressive Strength

To use MPC in practice, its compressive strength should be examined. Considering that MPC develops its strength very quickly at an early age, the 1 d and 7 d compressive strength of the paste cubes were tested, and the results are reported in Table 11. The strength values were not particularly high, which is due to the high W/S ratio used in this study, as reported in Table 1. For all mixes, the compressive strength increased with age (from 1 d to 7 d), which agrees with the results reported in the literature [17]. The development of the strength, which has been widely investigated, is due to the continuous generation of the hydration product i.e., struvite. It should be noted that the strength of the Run 15 is not available, which is due to the break-down of the cubes caused by expansion. It can be noticed that the compressive strength varied with the change of the three factors, i.e., W/S Ratio ( $X_1$ ), M/P Ratio ( $X_2$ ) and borax dosage ( $X_3$ ), indicating the potential effects of these factors on compressive strength. The relationships between the strength and the rheologic parameters, as well as the interactions between the variables and their combined effects on the strength and rheologic properties will be investigated in future.

**Table 11.** The compressive strength of the cube specimens.

Runs	1 d Compressive Strength/MPa	7 d Compressive Strength/MPa
1	23.7	34.6
2	33.8	34.4
3	19.1	39.0
4	21.8	32.2
5	23.3	33.2
6	22.4	33.8
7	27.5	43.1
8	29.2	32.3
9	13.7	15.8
10	9.2	10.6



Table 11. Cont.

Runs	1 d Compressive Strength/MPa	7 d Compressive Strength/MPa
11	21.0	30.8
12	18.5	22.8
13	21.7	22.9
14	21.5	31.9
15	n.a.	n.a.
16	21.7	32.8
17	11.1	11.6
18	19.9	27.2
19	10.2	14.1
20	7.2	8.2

#### 4. Conclusions

Based on the results obtained, the following conclusions can be drawn:

- The RSM-CCD methodology was successfully adopted to investigate the rheological behaviour of MPC material and to optimise the mix proportion in terms of W/S, M/P and borax dosage, with initial mini slump, mini-slump loss, yield stress and plastic viscosity considered as responses.
- The W/S ratio was identified as the significant factor (95% confidence level) affecting the plastic viscosity and the initial mini slump. The increase in W/S led to the decrease in the plastic viscosity, whereas it increased the mini slump. Moreover, the influence on the yield stress could not be ignored, since it remained at a 90% confidence level.
- The yield stress and mini-slump loss were influenced by the M/P ratio. The increase in the M/P ratio was shown to increase the yield stress and mini-slump loss.
- Borax dosage clearly affected the yield stress and mini-slump loss of MPC. With the increase in borax dosage, the yield stress and mini-slump loss decreased.
- The numerical optimisation showed that the best predicted values for the four responses are 0.680 Pa (yield stress), 0.263 Pa·s (plastic viscosity), 161.858 mm (initial mini slump) and 11.282 (mini-slump loss), with the desirability of 0.867.

**Author Contributions:** Conceptualization, Y.Y., J.Q. and Y.B.; data curation, Y.Y. and J.R.; formal analysis, J.R., K.Y. and D.W.; funding acquisition, J.Q. and Y.B.; investigation, Y.Y.; methodology, Y.Y. and J.R.; project administration, Y.Y.; supervision, J.Q. and Y.B.; validation, Y.Y.; visualization, J.R., K.Y. and D.W.; writing—original draft, Y.Y.; writing—review and editing, J.R. All authors have read and agreed to the published version of the manuscript.

**Funding:** This research was funded by the UK Engineering and Physical Sciences Research Council (EPSRC) (grant number EP/M003159/1) and the National Natural Science Foundation of China (NSFC) (grant number 51461135003) under the EPSRC-NSFC Collaborative Research Scheme on ‘Sustainable Materials for Infrastructure’.

**Institutional Review Board Statement:** Not applicable.

**Informed Consent Statement:** Not applicable.

**Data Availability Statement:** Data are contained within the article.

**Acknowledgments:** The authors would like to acknowledge Richard Baker Harrison Ltd. for providing magnesium oxide (MgO) for this research.

**Conflicts of Interest:** The authors declare no conflict of interest.

## References

1. Qin, J.H.; Qian, J.S.; You, C.; Fan, Y.R.; Zhen, W. Bond behavior and interfacial micro-characteristics of magnesium phosphate cement onto old concrete substrate. *Constr. Build. Mater.* **2018**, *167*, 166–176. [\[CrossRef\]](#)
2. Yang, Q.; Zhu, B.; Wu, X. Characteristics and durability test of magnesium phosphate cement-based material for rapid repair of concrete. *Mater. Struct.* **2000**, *33*, 229–234. [\[CrossRef\]](#)
3. Qiao, F.; Chau, C.K.; Li, Z. Property evaluation of magnesium phosphate cement mortar as patch repair material. *Constr. Build. Mater.* **2010**, *24*, 695–700. [\[CrossRef\]](#)
4. Sun, W.; Zheng, Y.; Zhou, L.; Song, J.; Bai, Y. A study of the bond behavior of FRP bars in MPC seawater concrete. *Adv. Struct. Eng.* **2020**, *24*, 1110–1123. [\[CrossRef\]](#)
5. Ma, H.Y.; Xu, B.; Li, Z. Magnesium potassium phosphate cement paste: Degree of reaction, porosity and pore structure. *Cem. Concr. Res.* **2014**, *65*, 96–104. [\[CrossRef\]](#)
6. Mahmoud, A.A.; Elkatatny, S.; Al-Majed, A.; Ramadan, M.A. The use of graphite to improve the stability of Saudi class G oil-well cement against the carbonation process. *ACS. Omega* **2022**, *7*, 5764–5773. [\[CrossRef\]](#)
7. Seehra, S.S.; Gupta, S.; Kumar, S. Rapid setting magnesium phosphate cement for quick repair of concrete pavements—Characterisation and durability aspects. *Cem. Concr. Res.* **1993**, *23*, 254–266. [\[CrossRef\]](#)
8. Ma, H.Y.; Xu, B.; Liu, J.; Pei, H.; Li, Z. Effects of water content, magnesia-to-phosphate molar ratio and age on pore structure, strength and permeability of magnesium potassium phosphate cement paste. *Mater. Des.* **2014**, *64*, 497–502. [\[CrossRef\]](#)
9. Lai, Z.Y.; Wang, H.T.; Hu, Y.; Yan, T.; Lu, Z.Y. Rapid Solidification of Highly Loaded High-Level Liquid Wastes with Magnesium Phosphate Cement. *Ceram. Int.* **2018**, *45*, 5050–5057. [\[CrossRef\]](#)
10. Weng, Y.W.; Ruan, S.Q.; Li, M.Y.; Mo, L.W.; Unluer, C.; Tan, M.J.; Qian, S.Z. Feasibility study on sustainable magnesium potassium phosphate cement paste for 3D printing. *Constr. Build. Mater.* **2019**, *221*, 595–603. [\[CrossRef\]](#)
11. Abdelrazig, B.; Sharp, J.H.; El-Jazairi, B. The Chemical Composition of Mortars Made from Magnesia-Phosphate Cement. *Cem. Concr. Res.* **1988**, *18*, 415–425. [\[CrossRef\]](#)
12. You, C.; Qian, J.S.; Qin, J.H.; Wang, H.; Wang, Q.; Ye, Z. Effect of early hydration temperature on hydration product and strength development of magnesium phosphate cement (MPC). *Cem. Concr. Res.* **2015**, *78*, 179–189. [\[CrossRef\]](#)
13. Xu, B.W.; Lothenbach, B.; Leemann, A.; Winnefeld, F. Reaction mechanism of magnesium potassium phosphate cement with high magnesium-to-phosphate ratio. *Cem. Concr. Res.* **2018**, *108*, 140–151. [\[CrossRef\]](#)
14. Xu, B.W.; Winnefeld, F.; Kaufmann, J.; Lothenbach, B. Influence of magnesium-to-phosphate ratio and water-to-cement ratio on hydration and properties of magnesium potassium phosphate cements. *Cem. Concr. Res.* **2019**, *123*, 105781. [\[CrossRef\]](#)
15. Xu, B.W.; Ma, H.; Li, Z. Influence of magnesia-to-phosphate molar ratio on microstructures, mechanical properties and thermal conductivity of magnesium potassium phosphate cement paste with large water-to-solid ratio. *Cem. Concr. Res.* **2015**, *68*, 1–9. [\[CrossRef\]](#)
16. Qin, Z.H.; Ma, C.; Zheng, Z.Q.; Long, G.C.; Chen, B. Effects of metakaolin on properties and microstructure of magnesium phosphate cement. *Constr. Build. Mater.* **2020**, *234*, 117353. [\[CrossRef\]](#)
17. Li, Y.; Chen, B. Factors that affect the properties of magnesium phosphate cement. *Constr. Build. Mater.* **2013**, *47*, 977–983. [\[CrossRef\]](#)
18. Jia, X.W.; Li, J.M.; Wang, P.; Qian, J.S.; Tang, M.H. Preparation and mechanical properties of magnesium phosphate cement for rapid construction repair in ice and snow. *Constr. Build. Mater.* **2019**, *229*, 116927.1–116927.13. [\[CrossRef\]](#)
19. Wang, D.Q.; Yue, Y.F.; Mi, T.W.; Yang, S.Y.; Bai, Y. Effect of magnesia-to-phosphate ratio on the passivation of mild steel in magnesium potassium phosphate cement. *Corros. Sci.* **2020**, *174*, 108848. [\[CrossRef\]](#)
20. Banfill, P.F.G.; Teixeira, M.A.O.M.; Craik, R.J.M. Rheology and vibration of fresh concrete: Predicting the radius of action of poker vibrators from wave propagation. *Cem. Concr. Res.* **2011**, *41*, 932–941. [\[CrossRef\]](#)
21. Ribeiro, D.V.; Paula, G.R.; Morelli, M.R. Effect of boric acid content on the properties of magnesium phosphate cement. *Constr. Build. Mater.* **2019**, *214*, 557–564. [\[CrossRef\]](#)
22. Bezerra, M.A.; Santelli, R.E.; Oliveira, E.P.; Villar, L.S.; Escalera, L.A. Response surface methodology (RSM) as a tool for optimization in analytical chemistry. *Talanta* **2008**, *76*, 965–977. [\[CrossRef\]](#) [\[PubMed\]](#)
23. Ren, J.; Fang, Y.H.; Ma, Q.M.; Tan, H.B.; Wang, X.F. Effect of storage condition on basic performance of polycarboxylate superplasticiser system incorporated sodium gluconate. *Constr. Build. Mater.* **2019**, *223*, 852–862. [\[CrossRef\]](#)
24. Ren, J. Superplasticiser for NaOH-Activated Slag: Competition and Instability between Superplasticiser and Alkali-Activator. Ph.D. Thesis, University College London (UCL), London, UK, 2016.
25. Mohammed, S.J.M.; Luti, K.J.K. Response surface methodology: A review on its applications and challenges in microbial cultures. *Mater. Today-Proc.* **2021**, *42*, 2277–2284. [\[CrossRef\]](#)
26. Yolmeh, M.; Jafari, S.M. Applications of Response Surface Methodology in the Food Industry Processes. *Food. Bioprocess. Tech.* **2017**, *10*, 413–433. [\[CrossRef\]](#)
27. Zl, A.; Dlab, C.; Xga, B. Multi-objective optimization of gap-graded cement paste blended with supplementary cementitious materials using response surface methodology. *Constr. Build. Mater.* **2020**, *248*, 118552. [\[CrossRef\]](#)
28. Ghafari, E.; Costa, H.; Júlio, E. Statistical mixture design approach for eco-efficient UHPC. *Cem. Concr. Compos.* **2015**, *55*, 17–25. [\[CrossRef\]](#)

29. Sonebi, M.; Abdalqader, A.; Fayyad, T.; Perrot, A.; Bai, Y. Optimisation of rheological parameters, induced bleeding, permeability and mechanical properties of supersulfated cement grouts. *Constr. Build. Mater.* **2020**, *262*, 120078. [[CrossRef](#)]
30. Sonebi, M.; Lachemi, M.; Hossain, K. Optimisation of rheological parameters and mechanical properties of superplasticised cement grouts containing metakaolin and viscosity modifying admixture. *Constr. Build. Mater.* **2013**, *38*, 126–138. [[CrossRef](#)]
31. Hou, D.; Chen, D.; Wang, X.; Wu, D.; Yu, R. RSM-based modelling and optimization of magnesium phosphate cement-based rapid-repair materials. *Constr. Build. Mater.* **2020**, *263*, 120190. [[CrossRef](#)]
32. Yue, Y.F.; Hu, W.Y.; You, C.; Qian, J.H.; McCague, C.; Jin, F.; Al-Tabbaa, A.; Mo, L.W.; Deng, M.; Bai, Y. A Statistical Investigation of the Rheological Properties of Magnesium Phosphate Cement. In Proceedings of the International Workshop on Innovation in Low-Carbon Cement & Concrete Technology, London, UK, 21–24 September 2016.
33. Lahalle, H.; Coumes, C.C.D.; Mercier, C.; Lambertin, D.; Gauffinet, S. Influence of the w/c ratio on the hydration process of a magnesium phosphate cement and on its retardation by boric acid. *Cem. Concr. Res.* **2018**, *109*, 159–174. [[CrossRef](#)]
34. Robert, J.; Flatt, R. Dispersion forces in cement suspensions. *Cem. Concr. Res.* **2004**, *34*, 399–408. [[CrossRef](#)]
35. Perrot, A.; Lecompte, T.; Khelifi, H.; Brumaud, C.; Hot, J.; Roussel, N. Yield stress and bleeding of fresh cement pastes. *Cem. Concr. Res.* **2012**, *42*, 937–944. [[CrossRef](#)]
36. Rubio-Hernández, F.; Adarve-Castro, A.; Velázquez-Navarro, J.; Páez-Flor, N.; Delgado-García, R. Influence of water/cement ratio, and type and concentration of chemical additives on the static and dynamic yield stresses of Portland cement paste. *Constr. Build. Mater.* **2020**, *235*, 117744. [[CrossRef](#)]
37. Struble, L.J.; Lei, W.G. Rheological changes associated with setting of cement paste. *Adv. Cem. Based. Mater.* **1995**, *2*, 224–230. [[CrossRef](#)]
38. Lu, Z.; Hou, D.; Ma, H.; Fan, T.; Li, Z. Effects of graphene oxide on the properties and microstructures of the magnesium potassium phosphate cement paste. *Constr. Build. Mater.* **2016**, *119*, 107–112. [[CrossRef](#)]
39. Le Rouzic, M.; Chaussadent, T.; Platret, G.; Stefan, L. Mechanisms of k-struvite formation in magnesium phosphate cements. *Cem. Concr. Res.* **2017**, *91*, 117–122. [[CrossRef](#)]
40. Zhang, X.; Hu, J.; Spanjers, H.; Lier, J.B.V. Struvite crystallization under a marine/brackish aquaculture condition. *Bioresour. Technol.* **2016**, *218*, 1151–1156. [[CrossRef](#)]
41. Moseke, C.; Saratsis, V.; Gbureck, U. Injectability and mechanical properties of magnesium phosphate cements. *J. Mater. Sci. Mater. Med.* **2011**, *22*, 2591–2598. [[CrossRef](#)]
42. Feng, P.; Zhou, S.G.; Zhao, J. Effect of cattle manure ash on workability and mechanical properties of magnesium phosphate cement. *Constr. Build. Mater.* **2016**, *129*, 79–88. [[CrossRef](#)]
43. Lahalle, H.; Céline, C.; Mesbah, A.; Lambertin, D.; Cannes, C.; Delpech, S.; Gauffinet, S. Investigation of magnesium phosphate cement hydration in diluted suspension and its retardation by boric acid. *Cem. Concr. Res.* **2016**, *87*, 77–86. [[CrossRef](#)]